

Perfect Excitation of Topological States by Supersymmetric Waveguides

Xuanyu Liu,^{*} Zhiyuan Lin,^{*} Wange Song^{✉,†}, Jiacheng Sun, Chunyu Huang, Shengjie Wu,
Xingjian Xiao, Haoran Xin, Shining Zhu[✉], and Tao Li^{✉‡}

*National Laboratory of Solid State Microstructures, Key Laboratory of Intelligent Optical Sensing and Manipulations,
Jiangsu Key Laboratory of Artificial Functional Materials, College of Engineering and Applied Sciences, School of Physics,
Nanjing University, Nanjing, 210093, China*



(Received 29 June 2023; accepted 20 November 2023; published 3 January 2024)

Topological photonic states provide intriguing strategies for robust light manipulations, however, it remains challenging to perfectly excite these topological eigenstates due to their complicated mode profiles. In this work, we propose to realize the exact eigenmode of the topological edge states by *supersymmetric* (SUSY) structures. By adiabatically transforming the SUSY partner to its main topological structure, the edge modes can be perfectly excited with simple single-site input. We experimentally verify our strategy in integrated silicon waveguides in telecommunication wavelength, showing a broad working bandwidth. Moreover, a *shortcut-to-adiabaticity* strategy is further applied to speed up the adiabatic pump process by *inverse-design* approaches, thus enabling fast mode evolutions and leading to reduced device size. Our method is universal and beneficial to the topology-based or complex eigenmodes systems, ranging from photonics and microwaves to cold atoms and acoustics.

DOI: [10.1103/PhysRevLett.132.016601](https://doi.org/10.1103/PhysRevLett.132.016601)

Photonic topological states have shown powerful capabilities for light manipulations [1–6]. These topological states are localized at the edge of two topologically inequivalent phases and possess unique properties, e.g., robustness against defects and disorders, which can be harnessed in photonic systems to achieve various applications, including the implementation of topological waveguiding [7–9], robust light routing [10–12], and lasing [13–15]. To fully utilize the property of the topological states, perfect excitation of the eigenmode is of vital importance, but is quite challenging due to the complicated mode distributions. Previous works usually adopted single-site input from the edge for simplicity, which deviates from the exact eigenmode and thus inevitably excites the bulk modes. These unwanted bulk modes would destroy the localization performance and lead to degraded performance.

Recently, the concept of supersymmetry (SUSY) was applied to optics [16,17], which was originally developed in the quantum field theory to establish a relation between bosons and fermions [18–22]. The SUSY transformation enables flexible designs on optical potential (i.e., refractive index) while generally preserving the eigenenergy spectrum, thus opening up new possibilities for futuristic optical devices that may be difficult to realize commonly, such as on-chip mode conversion [23–30], control of system scattering characteristics [31–34], and high-power single-mode laser array [35–37]. It is noteworthy that Queraltó *et al.* have proposed the combination of SUSY with topology, showcasing an intriguing mechanism for manipulating topological states [38]. However, to precisely excite the topological modes still remains a big challenge

and is seldom reported. In this regard, the design of SUSY with high flexibility in optical mode engineering would possibly provide us a feasible route to generate the accurate topological states.

In this Letter, we theoretically propose and experimentally demonstrate a supersymmetric route for topological state excitation in integrated photonic waveguides. Specifically, we design a SUSY partner based on the original topological structure that supports nontrivial edge states (e.g., the celebrated zero modes). It is found that through an appropriate adiabatic connection of topological structure and its SUSY partner, the single-site input waveguide mode in the SUSY partner can evolve robustly into the topological states of interest in broadband, which are further verified by experiments in silicon waveguide arrays. Moreover, we propose to utilize an inverse-design method to accelerate the adiabatic zero mode evolutions, which resembles the shortcut-to-adiabaticity (STA) process [39–42] and can lead to the excitation of edge states in a compact device. Our work illustrates the ability of supersymmetry to regulate topological modes, suggesting new possibilities for compact and broadband photonic devices.

We demonstrate our design principle based on the topological zero modes in the celebrated Su-Schrieffer-Heeger (SSH) model [43,44]. The SSH model is characterized by two sublattices with staggered weak (strong) couplings κ_1 (κ_2), and can host *zero-energy edge states* if the outermost coupling is weak. The topological zero states have nonzero projections in one of the sublattices due to the chiral symmetry. Single-mode optical waveguide arrays can be used to implement the SSH model through

evanescent field coupling [7,10,45,46]. If the overlap of evanescent fields in adjacent waveguides is small, the propagation of the optical field in the waveguide array can be described by the coupled mode theory (CMT) [47], which has a similar mathematic form to the Schrödinger equation:

$$-i \frac{d}{dz} \psi = H \psi, \quad (1)$$

where $\psi = (\psi_1, \dots, \psi_N)^T$ are the modal amplitudes in each waveguide and H is the system Hamiltonian featuring the propagation constants β_i in each waveguide (diagonal) and the couplings $\kappa_{i,i\pm 1}$ between them (off-diagonal). The mathematic form of SSH Hamiltonian H_{SSH} is shown in Ref. [48].

Discrete supersymmetry (DSUSY) transformations [17,23,38,49] can generate two supersymmetric partner Hamiltonians $H^{(1)}$ and $H^{(2)}$ with different but isospectral distributions. If supersymmetry is unbroken, $H^{(2)}$ will display an isolated site whose eigenvalue of the supported mode exactly corresponds to the one that desired to be removed [17,23,38,49]. Through the *QR factorization* (an efficient approach to factor a matrix as a product of two matrices traditionally called Q , R) [38,49,51], we can remove any desired eigenvalue from the supersymmetric partner, in other words, making it isolated corresponding to a single waveguide. The DSUSY transformation is implemented as follows [38,49]:

$$H_m^{(1)} - \mu_m I = QR \quad \text{and} \quad H_m^{(2)} - \mu_m I = RQ, \quad (2)$$

where I is the identity matrix, Q is an orthogonal matrix, and R is an upper triangular matrix. The QR factorization can be achieved using the *Givens rotation method* [51]. After applying a DSUSY transformation to the main topological structure H_{SSH} to remove the topological zero modes, the superpartner Hamiltonian H_{SUSY} can be obtained. Note there are multiple possible DSUSY transformations, among which we choose the H_{SUSY} that closely matches the SSH edge states [48].

Our model is implemented in the silicon-on-insulator (SOI) waveguides, as the schematics shown in the left panel of Fig. 1(a), where the input SUSY lattice adiabatically transforms into the output SSH lattice. Figure 1(b) shows the evolution of the mode constants (i.e., propagation constants) of the varying waveguides (left panel). Note there always exists a zero mode, which is located at a single waveguide at the SUSY input port and transforms into the eigenmode of a SSH zero mode at the output port (whose amplitude has a common ratio of $q = -\kappa_1/\kappa_2$ in interval sublattice, as shown in the upper right panel of Fig. 1(b)). Therefore, adiabatically transforming the SUSY structure into an SSH lattice can evolve the input single-site zero

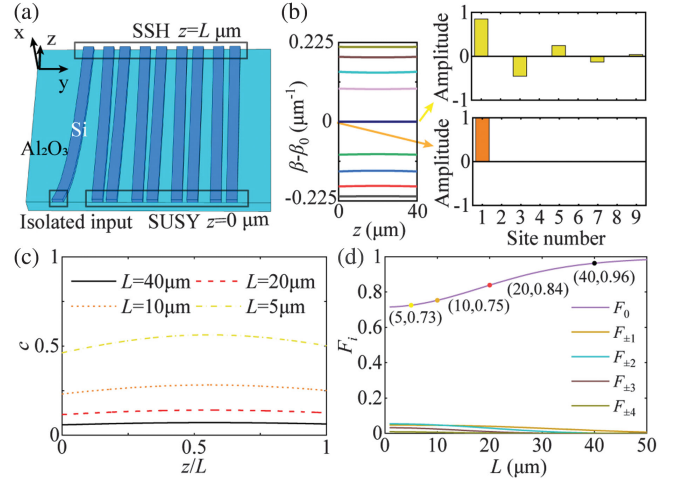


FIG. 1. (a) Schematics of the designed waveguide lattice that is adiabatically varying from SUSY ($z = 0$) to the SSH ($z = L$) lattices. L is the length of the waveguides. (b) Left panel: mode spectrum evolutions in the modulated waveguide lattice. The total waveguide number $N = 9$. Right panel: amplitude profile of the zero modes at $z = 0$ and $z = L$. (c) Adiabatic parameter c as a function of propagation length z/L . (d) Fidelity of the zero mode (F_0) and the overlap with bulk modes (F_i , where $i = -4, -3, -2, -1, 1, 2, 3, 4$ is the mode number) as a function of waveguide length L . $\kappa_1 = 0.0774 \mu\text{m}^{-1}$, $\kappa_2 = 0.1447 \mu\text{m}^{-1}$.

modes into the SSH zero modes. Here we assume the following modulation on the waveguide lattice:

$$\kappa_i(z) = g(z)\kappa_{\text{SSH},i} + (1 - g(z))\kappa_{\text{SUSY},i}, \quad (3)$$

where $\kappa_{\text{SUSY},i}$ and $\kappa_{\text{SSH},i}$ represent coupling coefficients in the input- and output-ports, respectively. The modulation function $g(z)$ should satisfy the condition $g(z) \in [0, 1]$, and $g(0) = 0$, $g(L) = 1$. Apparently, $g'(z)$ represents the change rate of the structure. For simplicity, we choose a linear modulation $g(z) = z/L$, which satisfies $g'(z) = \text{const}$ to make sure the SUSY array undergoes uniform variations at a steady rate.

Note that our design requires the adiabatic condition, i.e., the structure parameters should be slowly varied to ensure that the input zero mode evolves along the zero-energy band. Here, we define an *adiabatic parameter* c to measure if the adiabatic condition can be satisfied [52]:

$$c = \left| \frac{\langle \Psi_m | \frac{\partial}{\partial z} | \Psi_n \rangle}{\beta_m - \beta_n} \right|, \quad (4)$$

where the numerator and denominator represent the strength of *Berry connection* and the energy gap between bands m and n , respectively. A small value of an adiabatic parameter ($c \ll 1$) indicates the adiabatic condition can be satisfied. Figure 1(c) shows the adiabatic parameter between the zero mode band ($m = 0$) and the nearest-neighbor bulk band ($n = \pm 1$) of the SUSY array. It is found

that a shorter system has a larger c , thus making the adiabatic condition more difficult to be satisfied. To characterize the quality of the output zero modes (i.e., the efficiency of topological states pumps), we define the fidelity:

$$F = |\langle \Phi_0 | \psi(L) \rangle|^2, \quad (5)$$

where Φ_0 is the exact eigenmode of the SSH zero states we aim to produce and $\psi(L)$ is the actual output state. As shown in Fig. 1(d), the calculated fidelity is larger than 95% for $L > 36.3 \mu\text{m}$, where the adiabaticity can be well preserved. In contrast, the fidelity without the SUSY structure (i.e., with direct single-waveguide input to the SSH array) is only 71.5% under the same conditions [48].

To clearly visualize the zero mode pumping process, we carried out full-wave simulations of the light propagations in the SSH lattices with adiabatically varying SUSY as inputs [see Fig. 2(a)], and with direct single waveguide input to the edge of the SSH lattice as a comparison [Fig. 2(b)]. For direct single waveguide input, some light penetrates into the bulk, and the output state is not well localized at the edge and has undesired phase distributions [Fig. 2(b)]. In contrast, input from the SUSY case can excite the accurate supermodes, which is reflected in the subsequent SSH array with robust light field propagation and relatively accurate output [Fig. 2(a)].

In experiments, samples were fabricated using the method of E -beam lithography (EBL, Eliomix ELS-F125) and dry etching (OXFORD PP100) process, which include the waveguide array(s), an input grating coupler, and extended output ports (five outmost waveguides). The light was input into the waveguide lattice by focusing the laser ($\lambda = 1550 \text{ nm}$) via an input grating coupler. The transmitted light is scattered from the extended output ports and can be collected. The coupling-in and coupling-out processes were imaged by a near-infrared charge coupled device (CCD) camera, which is displayed in Fig. 2(e). We extracted the normalized intensity (I , red bars) of SSH lattice with SUSY displayed in Fig. 2(c), which agrees well with the simulation results (blue bars), confirming that the adiabatically varying SUSY array can almost produce the exact eigenmode of the zero states. As a comparison, the normalized output intensity of the single waveguide input case shows relatively poor locality and indicates more deviations from the exact zero mode [Fig. 2(d)]. Besides, the quantitative agreement between simulation and experiment is not as good as in the case with SUSY. This is because the fabrication imperfections significantly affect the optical transport of bulk modes (which will also be excited by single-waveguide input), whereas the topologically protected zero state propagates immune to them. Moreover, we can also employ a similar design principle to generate the topological interface modes of the SSH lattice [48].

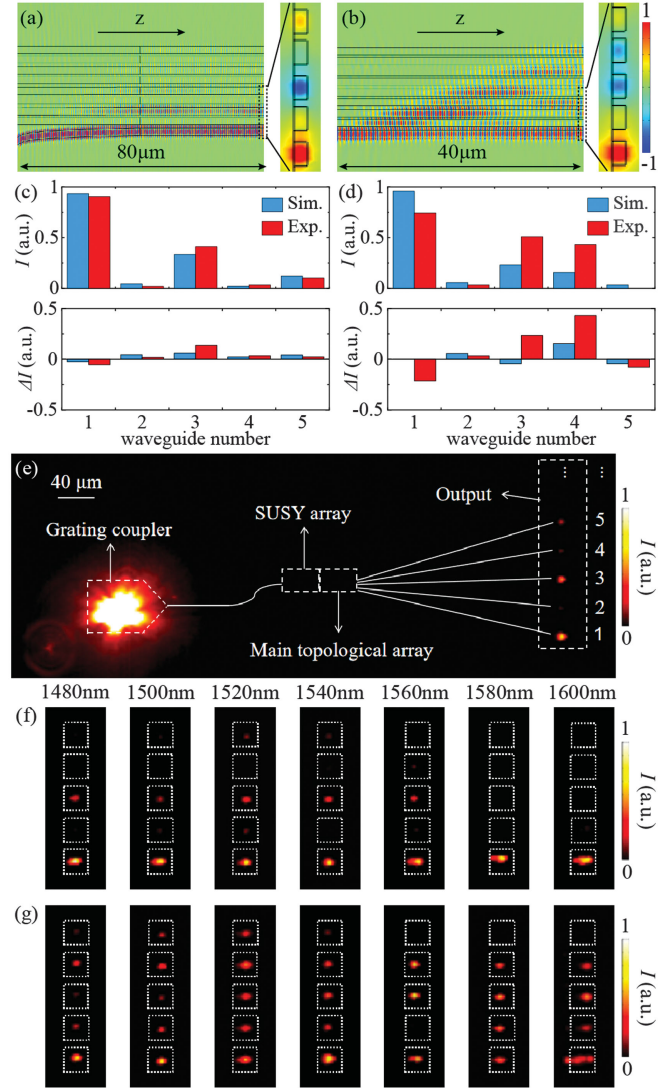


FIG. 2. (a),(b) Simulated light propagation (Ex) in the SSH lattices and corresponding output distributions with SUSY as front-end input (a) and with single-waveguide input (b). The waveguide width $w = 400 \text{ nm}$, height $h = 220 \text{ nm}$, supporting only one fundamental TE mode at $\lambda = 1550 \text{ nm}$ with propagation constant $\beta_0 = 2.1612k_0$, where k_0 is the free space k wave number. The gaps $d_{1(2)} = 200(120) \text{ nm}$ corresponding to coupling coefficients $\kappa_{1(2)} = 0.0774(0.1447) \mu\text{m}^{-1}$. (c),(d) Top: simulated (blue bars) and experimentally measured (red bars) output intensity profiles (I) with (c) and without (d) SUSY structure. Bottom: deviations from the exact zero modes (ΔI , bottom panels). (e) CCD recorded optical propagation in the waveguide lattice with SUSY structure. (f),(g) Wavelength-dependent behavior of the output of SSH array with (f) and without (g) SUSY.

Moreover, it is expected that the device can work in a broadband manner due to the adiabaticity of the structure. Here, we provide the experimentally measured output intensities of different wavelengths (1480, 1500, 1520, 1540, 1560, 1580, and 1600 nm). As shown in Fig. 2(f), the output modes with SUSY design exhibit similar intensity

distributions across an extremely wide wavelength range. In contrast, the output intensities with single-waveguide edge input are greatly influenced by the input wavelength [see Fig. 2(g)], all deviating from the eigen zero mode distributions [48].

The aforementioned SUSY design requires adiabatic conditions, which inevitably leads to a large device footprint (e.g., 40 μm in Fig. 2). Inspired by the shortcut to adiabaticity (STA) technique proposed in quantum physics to speed up the quantum state transfer [39–42], here we employ a similar accelerating process by inverse-design approaches [53,54] that can produce the same final state in a shorter length. Specifically, if the input and output of the waveguides are fixed and the length L is determined, the fidelity would be solely determined by a generalized modulation function $g(z)$:

$$g(z) = g_{\text{linear}} + g_F = \frac{z}{L} + \sum_{n=1}^N a(n) \sin \frac{2\pi n z}{L}, \quad (6)$$

where g_F is a half-range Fourier series. Note here $g(z)$ should be centrally symmetric about the point $(L/2, 1/2)$ as required by the symmetry of the SUSY array [48]. Using computational inverse-design approaches [53,54], we achieve the optimal fidelity F_{max} for different lengths under the constraint of $g(z) \in [0, 1]$ [48], as shown in Fig. 3(a). It is evident that the optimized SUSY arrays can significantly reduce the required length for the same fidelity (e.g., from 36 to 18 μm for $F = 0.945$). In this situation, the adiabaticity is destroyed and the zero modes are allowed to couple to other bulk modes. But finally they will get back to the zero-energy band and reproduce the desired topological zero modes [see blue curve in

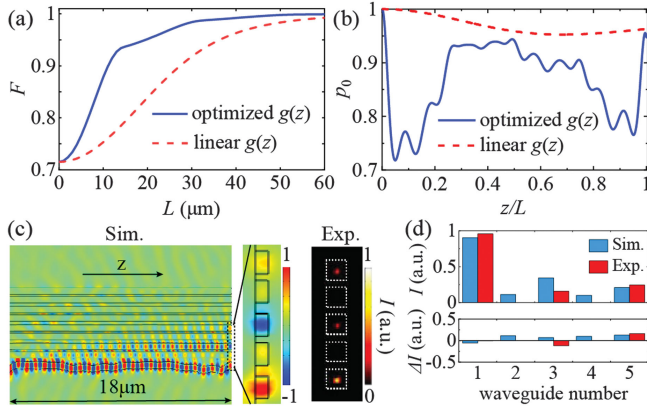


FIG. 3. (a) Fidelity of the zero modes for increasing device length. (b) Proportion of the zero mode (p_0) as a function of propagation length z/L [$L = 18 \mu\text{m}$ for optimized $g(z)$ and $40 \mu\text{m}$ for linear $g(z)$]. (c) Left panel: simulated light propagation (E_x distributions) and corresponding output distribution for the optimized SUSY array. Right panel: CCD recorded output signals in experiments. $L = 18 \mu\text{m}$. (d) Normalized intensity profiles of the outputs (top panel) and deviations from the exact zero mode (bottom panel).

Fig. 3(b)]. The simulation and experiment results further confirmed the theoretical analysis, as shown in Figs. 3(c) and 3(d), where the output still maintains a relatively accurate zero mode with good locality for $L = 18 \mu\text{m}$. The SUSY structure can efficiently and compactly excite topological states, enabling robust control of light propagation, which holds significant importance for quantum state manipulation [55] and photonic integration [7,10].

Having shown the excellent performance of the SUSY structure, we anticipate that these results are also robust against structural perturbations. In fact, due to the fulfillment of the adiabatic condition, the SUSY design still outperforms the single-waveguide input significantly even under a higher disorder strength, which remains acceptable even after STA acceleration [48].

In conclusion, we have exploited the topological zero mode pumps in adiabatic SUSY structure to perfectly excite the eigenmode of a topological state. Our strategy is universal to generate other topological states in different systems. As a proof of concept, we apply SUSY transformations to the SSH lattices hosting topological zero states. Adiabatically connecting the topological array and its SUSY partner enables the single-site zero mode to evolve robustly into the topological states of interest in broadband. Furthermore, we develop a STA-like strategy to accelerate the pumping process by inverse-design approaches, effectively making the device more compact. The experimental results in silicon waveguide arrays are fully consistent with our expectations. Our work demonstrates the superior capability of supersymmetry in regulating topological states, which provides a general approach to generating the topological modes, suggesting new possibilities in exploring topology-based effects and applications in compact photonic integrations. It is worth mentioning that the method demonstrated here may be extended to achieve perfect excitation of higher-dimensional photonic topological states, and even can be possibly applied to other systems, such as microwaves [56,57], acoustics [58,59], and ultracold atoms [60–63].

The authors acknowledge the financial support from The National Key R&D Program of China (2022YFA1404301, 2023YFA1407700), National Natural Science Foundation of China (No. 12174186, No. 12204233, No. 62325504, No. 62288101, No. 92250304), and Innovation and Entrepreneurship Program of Jiangsu Province (JSSCBS20220040). Tao Li thanks to the support from the Dengfeng Project B of Nanjing University.

*These authors contributed equally to this work.

†Corresponding author: songwange@nju.edu.cn

‡Corresponding author: taoli@nju.edu.cn

[1] L. Lu, J. D. Joannopoulos, and M. Soljačić, Topological photonics, *Nat. Photonics* **8**, 821 (2014).

- [2] T. Ozawa *et al.*, Topological photonics, *Rev. Mod. Phys.* **91**, 015006 (2019).
- [3] L. Lu, J. D. Joannopoulos, and M. Soljačić, Topological states in photonic systems, *Nat. Phys.* **12**, 626 (2016).
- [4] A. B. Khanikaev and G. Shvets, Two-dimensional topological photonics, *Nat. Photonics* **11**, 763 (2017).
- [5] T. Ozawa and H. M. Price, Topological quantum matter in synthetic dimensions, *Nat. Rev. Phys.* **1**, 349 (2019).
- [6] Y. Yang, Z. Gao, H. Xue, L. Zhang, M. He, Z. Yang, R. Singh, Y. Chong, B. Zhang, and H. Chen, Realization of a three-dimensional photonic topological insulator, *Nature (London)* **565**, 622 (2019).
- [7] A. Blanco-Redondo, I. Andonegui, M. J. Collins, G. Harari, Y. Lumer, M. C. Rechtsman, B. J. Eggleton, and M. Segev, Topological optical waveguiding in silicon and the transition between topological and trivial defect states, *Phys. Rev. Lett.* **116**, 163901 (2016).
- [8] X. T. He, E. T. Liang, J. J. Yuan, H. Y. Qiu, X. D. Chen, F. L. Zhao, and J. W. Dong, A silicon-on-insulator slab for topological valley transport, *Nat. Commun.* **10**, 872 (2019).
- [9] M. I. Shalaev, W. Walasik, A. Tsukernik, Y. Xu, and N. M. Litchinitser, Robust topologically protected transport in photonic crystals at telecommunication wavelengths, *Nat. Nanotechnol.* **14**, 31 (2019).
- [10] W. Song, W. Sun, C. Chen, Q. Song, S. Xiao, S. Zhu, and T. Li, Robust and broadband optical coupling by topological waveguide arrays, *Laser Photonics Rev.* **14**, 1900193 (2020).
- [11] Y. Wang, W. Liu, Z. Ji, G. Modi, M. Hwang, and R. Agarwal, Coherent interactions in one-dimensional topological photonic systems and their applications in all-optical logic operation, *Nano Lett.* **20**, 8796 (2020).
- [12] L. Sun, H. Wang, Y. He, Y. Zhang, G. Tang, X. He, J. Dong, and Y. Su, Broadband and fabrication tolerant power coupling and mode-order conversion using thouless pumping mechanism, *Laser Photonics Rev.* **16**, 2200354 (2022).
- [13] P. St-Jean, V. Goblot, E. Galopin, A. Lemaître, T. Ozawa, L. Le Gratiet, I. Sagnes, J. Bloch, and A. Amo, Lasing in topological edge states of a one-dimensional lattice, *Nat. Photonics* **11**, 651 (2017).
- [14] M. Parto, S. Wittek, H. Hodaei, G. Harari, M. A. Bandres, J. Ren, M. C. Rechtsman, M. Segev, D. N. Christodoulides, and M. Khajavikhan, Edge-mode lasing in 1d topological active arrays, *Phys. Rev. Lett.* **120**, 113901 (2018).
- [15] H. Zhao, P. Miao, M. H. Teimourpour, S. Malzard, R. El-Ganainy, H. Schomerus, and L. Feng, Topological hybrid silicon microlasers, *Nat. Commun.* **9**, 981 (2018).
- [16] M.-A. Miri, M. Heinrich, and D. N. Christodoulides, Supersymmetry-generated complex optical potentials with real spectra, *Phys. Rev. A* **87**, 043819 (2013).
- [17] M. A. Miri, M. Heinrich, R. El-Ganainy, and D. N. Christodoulides, Supersymmetric optical structures, *Phys. Rev. Lett.* **110**, 233902 (2013).
- [18] A. Neveu and J. H. Schwarz, Factorizable dual model of pions, *Nucl. Phys.* **B31**, 86 (1971).
- [19] P. Ramond, Dual theory for free fermions, *Phys. Rev. D* **3**, 2415 (1971).
- [20] D. V. Volkov and V. P. Akulov, Is the neutrino a goldstone particle?, *Phys. Lett.* **46B**, 109 (1973).
- [21] J. Wess and B. Zumino, Supergauge transformations in four dimensions, *Nucl. Phys.* **B70**, 39 (1974).
- [22] E. Witten, Dynamical breaking of supersymmetry, *Nucl. Phys.* **B188**, 513 (1981).
- [23] M. Heinrich, M. A. Miri, S. Stutzer, R. El-Ganainy, S. Nolte, A. Szameit, and D. N. Christodoulides, Supersymmetric mode converters, *Nat. Commun.* **5**, 3698 (2014).
- [24] M. Principe, G. Castaldi, M. Consales, A. Cusano, and V. Galdi, Supersymmetry-inspired non-Hermitian optical couplers, *Sci. Rep.* **5**, 8568 (2015).
- [25] G. Queralto, V. Ahufinger, and J. Mompert, Mode-division (de)multiplexing using adiabatic passage and supersymmetric waveguides, *Opt. Express* **25**, 27396 (2017).
- [26] A. Macho, R. Llorente, and C. García-Meca, Supersymmetric transformations in optical fibers, *Phys. Rev. Appl.* **9**, 014024 (2018).
- [27] G. Queralto, V. Ahufinger, and J. Mompert, Integrated photonic devices based on adiabatic transitions between supersymmetric structures, *Opt. Express* **26**, 33797 (2018).
- [28] W. Walasik, B. Midya, L. Feng, and N. M. Litchinitser, Supersymmetry-guided method for mode selection and optimization in coupled systems, *Opt. Lett.* **43**, 3758 (2018).
- [29] C. Huang and Q. Song, Guiding flow of light with supersymmetry, *Light Sci. Appl.* **11**, 290 (2022).
- [30] J. Yim, N. Chandra, X. Feng, Z. Gao, S. Wu, T. Wu, H. Zhao, N. M. Litchinitser, and L. Feng, Broadband continuous supersymmetric transformation: A new paradigm for transformation optics, *eLight* **2**, 16 (2022).
- [31] M. Heinrich, M. A. Miri, S. Stutzer, S. Nolte, D. N. Christodoulides, and A. Szameit, Observation of supersymmetric scattering in photonic lattices, *Opt. Lett.* **39**, 6130 (2014).
- [32] M.-A. Miri, M. Heinrich, and D. N. Christodoulides, SUSY-inspired one-dimensional transformation optics, *Optica* **1**, 89 (2014).
- [33] S. Longhi, Supersymmetric transparent optical intersections, *Opt. Lett.* **40**, 463 (2015).
- [34] C. Garcia-Meca, A. M. Ortiz, and R. L. Saez, Supersymmetry in the time domain and its applications in optics, *Nat. Commun.* **11**, 813 (2020).
- [35] M. P. Hokmabadi, N. S. Nye, R. El-Ganainy, D. N. Christodoulides, and M. Khajavikhan, Supersymmetric laser arrays, *Science* **363**, 623 (2019).
- [36] B. Midya, H. Zhao, X. Qiao, P. Miao, W. Walasik, Z. Zhang, N. M. Litchinitser, and L. Feng, Supersymmetric microring laser arrays, *Photonics Res.* **7**, 363 (2019).
- [37] X. Qiao, B. Midya, Z. Gao, Z. Zhang, H. Zhao, T. Wu, J. Yim, R. Agarwal, N. M. Litchinitser, and L. Feng, Higher-dimensional supersymmetric microlaser arrays, *Science* **372**, 403 (2021).
- [38] G. Queralto, M. Kremer, L. J. Maczewsky, M. Heinrich, J. Mompert, V. Ahufinger, and A. Szameit, Topological state engineering via supersymmetric transformations, *Commun. Phys.* **3**, 49 (2020).
- [39] X. Chen, I. Lizuain, A. Ruschhaupt, D. Guéry-Odelin, and J. G. Muga, Shortcut to adiabatic passage in two- and three-level atoms, *Phys. Rev. Lett.* **105**, 123003 (2010).
- [40] D. Guéry-Odelin, A. Ruschhaupt, A. Kiely, E. Torrontegui, S. Martínez-Garaot, and J. G. Muga, Shortcuts to adiabaticity:

- Concepts, methods, and applications, *Rev. Mod. Phys.* **91**, 045001 (2019).
- [41] N. N. Hegade, K. Paul, Y. Ding, M. Sanz, F. Albarrán-Arriagada, E. Solano, and X. Chen, Shortcuts to adiabaticity in digitized adiabatic quantum computing, *Phys. Rev. Appl.* **15**, 024038 (2021).
- [42] Z. Yin, C. Li, J. Allcock, Y. Zheng, X. Gu, M. Dai, S. Zhang, and S. An, Shortcuts to adiabaticity for open systems in circuit quantum electrodynamics, *Nat. Commun.* **13**, 188 (2022).
- [43] W. P. Su, J. R. Schrieffer, and A. J. Heeger, Solitons in polyacetylene, *Phys. Rev. Lett.* **42**, 1698 (1979).
- [44] A. J. Heeger, S. Kivelson, J. R. Schrieffer, and W. P. Su, Solitons in conducting polymers, *Rev. Mod. Phys.* **60**, 781 (1988).
- [45] W. Song, W. Sun, C. Chen, Q. Song, S. Xiao, S. Zhu, and T. Li, Breakup and recovery of topological zero modes in finite non-Hermitian optical lattices, *Phys. Rev. Lett.* **123**, 165701 (2019).
- [46] S. Xia, D. Kaltsas, D. Song, I. Komis, J. Xu, A. Szameit, H. Buljan, K. G. Makris, and Z. Chen, Nonlinear tuning of PT symmetry and non-Hermitian topological states, *Science* **372**, 72 (2021).
- [47] A. Yariv, Coupled-mode theory for guided-wave optics, *IEEE J. Quantum Electron.* **9**, 919 (1973).
- [48] See Supplemental Material at <http://link.aps.org/supplemental/10.1103/PhysRevLett.132.016601> for discussion about detailed SUSY transformations of a SSH lattice, the optimal SUSY partner, excitation of the SSH interface states, supplementary experimental results of the broadband performance, more details of accelerating the pumping process, and robustness analyses of the SUSY structure, which includes Refs. [7,33,38,49,50].
- [49] D. Viedma, G. Queralto, J. Mompart, and V. Ahufinger, High-efficiency topological pumping with discrete supersymmetry transformations, *Opt. Express* **30**, 23531 (2022).
- [50] Q. Cheng, Y. Pan, Q. Wang, T. Li, and S. Zhu, Topologically protected interface mode in plasmonic waveguide arrays, *Laser, Photonics Rev.* **9**, 392 (2015).
- [51] L. Hogben, *Handbook of Linear Algebra*, 2nd ed (Chapman & Hall/CRC, New York, 2013).
- [52] M. Born and V. Fock, Beweis des adiabatenatzes, *Z. Med. Phys.* **51**, 165 (1928).
- [53] S. Molesky, Z. Lin, A. Y. Piggott, W. Jin, J. Vucković, and A. W. Rodriguez, Inverse design in nanophotonics, *Nat. Photonics* **12**, 659 (2018).
- [54] L. Ma, J. Li, Z. Liu, Y. Zhang, N. Zhang, S. Zheng, and C. Lu, Intelligent algorithms: New avenues for designing nanophotonic devices, *Chin. Optic. Lett.* **19**, 011301 (2021).
- [55] A. Blanco-Redondo, B. Bell, D. Oren, B. J. Eggleton, and M. Segev, Topological protection of biphoton states, *Science* **362**, 568 (2018).
- [56] Q. Cheng, Y. Pan, H. Wang, C. Zhang, D. Yu, A. Gover, H. Zhang, Tao Li, L. Zhou, and S. N. Zhu, Observation of anomalous π modes in photonic Floquet engineering, *Phys. Rev. Lett.* **122**, 173901 (2019).
- [57] Q. Cheng, H. Wang, Y. Ke, T. Chen, Y. Yu, Y. S. Kivshar, C. Lee, and Y. Pan, Asymmetric topological pumping in nonparaxial photonics, *Nat. Commun.* **13**, 249 (2022).
- [58] Y.-X. Shen, Y.-G. Peng, D.-G. Zhao, X.-C. Chen, J. Zhu, and X.-F. Zhu, One-way localized adiabatic passage in an acoustic system, *Phys. Rev. Lett.* **122**, 094501 (2019).
- [59] O. You, S. Liang, B. Xie, W. Gao, W. Ye, J. Zhu, and S. Zhang, Observation of non-Abelian Thouless pump, *Phys. Rev. Lett.* **128**, 244302 (2022).
- [60] M. Atala, M. Aidelsburger, J. T. Barreiro, D. Abanin, T. Kitagawa, E. Demler, and I. Bloch, Direct measurement of the Zak phase in topological Bloch bands, *Nat. Phys.* **9**, 795 (2013).
- [61] L. Wang, M. Troyer, and X. Dai, Topological charge pumping in a one-dimensional optical lattice, *Phys. Rev. Lett.* **111**, 026802 (2013).
- [62] M. Lohse, C. Schweizer, O. Zilberberg, M. Aidelsburger, and I. Bloch, A Thouless quantum pump with ultracold bosonic atoms in an optical superlattice, *Nat. Phys.* **12**, 350 (2015).
- [63] S. Nakajima, T. Tomita, S. Taie, T. Ichinose, H. Ozawa, L. Wang, M. Troyer, and Y. Takahashi, Topological Thouless pumping of ultracold fermions, *Nat. Phys.* **12**, 296 (2016).